# OPTIMIZATION OF SURFACE ROUGHNESS AND MRR WHEN MILLING 25CRMO4-25 STEEL USING TAGUCHI DESIGN

**Mohamed Fnides[1], Salah Amroune[2], Barhm Mohamad[3*], Brahim Fnides[4], Bensana Toufik[1]**
[1]*Higher School of Technological Education in Skikda, Azzaba, Algeria*
[2]*Laboratoire de Matériaux et Mécanique des Structures (LMMS). Université de M'sila. Algérie*
[3]*Department of Petroleum Technology, Koya Technical Institute, Erbil Polytechnic University, 44001 Erbil, Iraq*
[4]*Université des Sciences et de la Technologie Houari Boumediene Bab-Ezzouar, Alger, Algérie Corresponding Email : barhm.mohamad@epu.edu.iq*

***ABSTRACT:*** *This study investigates the impact of cutting parameters—cutting speed (Vc), feed rate (fz), and depth of cut (ap)—on surface roughness (Ra) during the dry face milling of 25CrMo4-25 steel, using CT530 inserts and response surface methodology (RSM). Through a series of machining experiments based on statistically designed three-factor and four-level factorial experiment designs (Taguchi Design) and thorough statistical analysis of variance (ANOVA), a mathematical model was developed to identify significant factors influencing Ra. Moreover, a multi-objective optimization approach was applied to minimize Ra and maximize material removal rate (MRR) using a desirability approach. The resulting models established the relationships between cutting parameters (Vc, fz, and ap) and Ra. The analysis revealed the significance of the mathematical model for Ra (R2 = 96.61%), enabling reliable prediction of surface roughness during machining of 25CrMo4-25 steel. Notably, the study found that the feed rate had the most significant impact on Ra (53.95%), followed by cutting speed contributing 38.75% to Ra. Conversely, the depth of cut had a negligible effect.*

***KEYWORDS****: Modeling, Taguchi, Surface Roughness, ANOVA.*

## 1. INTRODUCTION

In the realm of machining, both modeling and optimization tasks hold significant importance [1-5]. They enable the selection of optimal cutting conditions to achieve desired outcomes, often with direct economic implications such as machine time and total operational cost. Within manufacturing processes, especially in machining, the quality of surfaces produced is pivotal in determining integrity levels [6-8]. Among various machining techniques employed in manufacturing industries, milling stands out as one of the most prevalent due to its capability to swiftly remove material while maintaining reasonably good surface quality [9-12].

The Response Surface Methodology (RSM) serves as a general approach to maximizing the value of a dependent variable by considering several independent variables. Key parameters like surface roughness and material removal rate (MRR) significantly impact the machining process [13-16]. For instance, researchers Parida and Maity [17] introduced a modeling technique for surface roughness and optimized cutting parameters to establish an optimal cutting regime, aiming to minimize roughness and maximize MRR during AISI 1040 steel machining.

Similarly, other researchers Marichamy et al. [18] optimized cutting parameters (Vc, fz, and ap) and modeled results such as MRR, surface roughness, cutting force, and tool tip temperature when machining Incoloy 800H, employing Taguchi-based Gray's Relational Analysis (GRA) and Response Surface Methodology (RSM). This technique combines the design of experiments (COE) and multiple regressions to ascertain the form of influence, be it linear, quadratic, cubic, etc., and the mathematical equation governing the phenomenon's variation with precision [19-22].

The modeling process involves selecting experimental points, typically equal to or greater than the sum of effects, interactions, and quadratic effects, to define a matrix of n rows and k columns, where n represents the number of experiments and k denotes the number of effects. Our work aligns with this methodology. Notably, a study by Ghosh et al. [23] demonstrates strong agreement between experimental and predicted Ra values for the RSM-PSO technique during modeling and optimizing cutting parameters

for keyway milling operations of C40 steel under wet conditions.

Furthermore, in the context of face milling AISI 1045 Steel, Trung [24] suggested two models for predicting surface roughness—one based on the Johnson transformation and the other developed using Response Surface Methodology (RSM). Regarding the machinability of AISI 5140 steel. Kuntoğlu et al. [25] conducted a study to determine optimal cutting conditions, analyze vibrations, and assess surface roughness under varying cutting parameters.

Moreover, employing neural network methods, Sureshkumar et al. [26] investigated the influence of cutting parameters (vc, fz, and ap) on surface roughness in milling operations. Ultimately, modeling and optimization serve crucial roles in selecting optimal cutting regimes during machining to achieve desired outcomes [27].

Bouzid et al. [28] determined optimal values for minimizing surface roughness and maximizing material removal rate (MRR) during the turning of X20Cr13 stainless steel. Their study concluded that a feed rate of 0.08 mm/rev, a depth of cut of 0.15 mm, and a cutting speed of 120 m/min yield the best results.

In another experimental investigation, Pandiyan & Prabaharan et al. [29] evaluated the machining of AA6351 alloy steel using a CNC machining center. They employed Response Surface Methodology (RSM) along with objective functions and optimization methods to identify process variable values that yield desirable responses. Mathematical models were developed based on the obtained responses and were subsequently validated.

## 2. MATERIALS AND METHODS

Presented are the different methods used for planning and the conditions for carrying out the experiments. Additionally, all the tools used to conduct the experiments are presented; this will consist of a presentation of various equipment that are used to monitor the evolution of the surfaces roughness during face milling. The experiments necessary for our study were carried out at the Laboratory of Mechanics and Structure (LMS), Department of Mechanics of the University of May 8, 1945 of Guelma.

The machine tool that was used for our tests is a vertical milling machine from the National Society for the Production of Industrial Machine Tools (PMO), model ALMO with a power of 5 KW (Fig. 1) on 25CrMo4-25 grade steel specimens (70x70x120) machined with four CT530 inserts (fig. 2) fixed on an 80 mm diameter face milling cutter (fig. 3). Spindle Rotational Speed available on the milling machine: 45; 63; 90; 125; 180; 250; 355; 500; 710; 1000, 1400; 2000.

The different feed rates of this machine are in (mm/min): 10; 16; 20, 25; 31.5, 50; 63; 80; 100; 125; 160; 200; 250; 314; 400; 500; 630; 800.

**Fig. 3. Machine Tools (PMO), model ALMO**


**Fig. 1. 4:Insert: CT530**


**Fig. 2. Coromill 245 face milling cutter**

### 2.1. Experiment planning and procedures

The constants and coefficients of the mathematical models were determined using Minitab and Design-Expert software, employing analysis of variance (ANOVA), multiple regressions, and the response surface method (RSM). Equation 1 in this study describes the relationship between the cutting conditions and the technological parameters.

$$Y = \varphi(Vc.fz.ap) \quad (1)$$

Where $\varphi$ is the response function, representing the approximation of Y, is formulated using a non-linear (quadratic) mathematical model. This model is chosen

for its suitability in analyzing the interaction effects of process parameters on machinability characteristics. In this study, Equation 2 presents the RSM-based second-order mathematical model.

$$Y = b_o + \sum_{i=1}^{k} b_i X_i + \sum_{ij}^{k} b_{ij} X_i X_j + \sum_{i=1}^{k} b_{ii} X_i^2 + \varepsilon_{ij}$$

$$\left(\varepsilon_{ij} = y_{ij} - \bar{y}_{ij}\right) \quad (2)$$

Chosen for the multi-factorial method are three factors and four levels, as presented in Table 1. The Taguchi design, specifically L16 runs, was selected for the design of experiments (DOE), with the experimental results provided in Table 2.

**Table 1. Factors and levels used in the experiments (Multi-factorial method)**

| Factors | Symbol | Levels | | | |
|---|---|---|---|---|---|
| | | Level 1 | Level 2 | Level 3 | Level 4 |
| Cutting speed (m/min) | Vc | 31,5 | 63 | 126 | 251 |
| Feed rate (mm/ tooth) | fz | 0.04 | 0.063 | 0.1 | 0.16 |
| Depth of cut (mm) | ap | 0.2 | 0.4 | 0.6 | 0.8 |

**Table 2. Experimental data for 25CrMo4-25 steel (Taguchi Design)**

| Runs | Vc, m/min | fz, mm/tooth | ap, mm | Ra, µm | Q, $Mm^3$/min |
|---|---|---|---|---|---|
| 1 | 31,5 | 0,04 | 0,2 | 3,949 | 707,85 |
| 2 | 31,5 | 0,063 | 0,4 | 5,153 | 1685,35 |
| 3 | 31,5 | 0,1 | 0,6 | 6,345 | 3595,41 |
| 4 | 31,5 | 0,16 | 0,8 | 7,16 | 898,85 |
| 5 | 63 | 0,04 | 0,4 | 3,264 | 707,85 |
| 6 | 63 | 0,063 | 0,2 | 3,671 | 4494,27 |
| 7 | 63 | 0,1 | 0,8 | 5,395 | 5393,12 |
| 8 | 63 | 0,16 | 0,6 | 6,638 | 2696,56 |
| 9 | 126 | 0,04 | 0,6 | 3,088 | 5662,78 |
| 10 | 126 | 0,063 | 0,8 | 4,262 | 2247,13 |
| 11 | 126 | 0,1 | 0,2 | 5,314 | 7190,83 |
| 12 | 126 | 0,16 | 0,4 | 5,851 | 7162,29 |
| 13 | 251 | 0,04 | 0,8 | 1,181 | 8460,46 |
| 14 | 251 | 0,063 | 0,6 | 2,6 | 8952,87 |
| 15 | 251 | 0,1 | 0,4 | 3,292 | 7162,29 |
| 16 | 251 | 0,16 | 0,2 | 4,413 | 707,85 |

## 3. RESULTS AND DISCUSSION

Statistical data treatments proceed through two distinct steps. Initially, ANOVA is employed to discern the effects of each factor and their interactions. This is facilitated by generating response surface plots, which analyze two parameters at a time while holding the third constant. Subsequently, the focus shifts to modeling aspects utilizing RMS outputs in the second step.

### 3.1. Modeling using RSM Technique (ANOVA analysis)

ANOVA serves as a valuable tool for comprehending the impact of input parameters in machining processes through designed experiments. It aids in interpreting the output data by partitioning the total variation into components attributed to controlled factors and generated errors. The statistical significance of fitted quadratic models is evaluated using p-values and F-values derived from the ANOVA.

Within the ANOVA table, the p-value represents the probability, ranging from 0 to 1. When the p-value exceeds 0.05, the parameter is deemed insignificant; conversely, if the p-value is less than 0.05, the parameter is considered significant. Additionally, the squared sum (SS) is employed to estimate the deviation squared from the overall mean (Eq.3).

$$SS_f = \frac{N}{N_{nf}} \sum_{i=1}^{N_{nf}} (\bar{y}_i - \bar{y})^2 \quad (3)$$

Where:

$\bar{y}$ : The average response.

$\bar{y}_i$ : The average of the measured responses for each level i of the f-factor.

N : the total number of trials.

Nnf : the number of levels of each f factor

The squared mean (MS) is calculated by dividing the squared sum by the number of degrees of freedom. (Eq.4).

$$MC_i = \frac{SS_i}{dl_i} \quad (4)$$

The F-value plays a crucial role in assessing the compatibility of the mathematical model. It is essential that the calculated F-values surpass the tabulated F from the F-Table for the model to be deemed compatible (Eq.5).

$$F_i = \frac{MC_i}{MC_e} \quad (5)$$

Where: MCe represent the mean squared sum of the errors.

In the ANOVA table, the "Cont%" column displays the contribution of factors as a percentage of the total variance, indicating the degree of percent effect on the response (Eq.6):

$$Cont.\% = \frac{SS_f}{SS_T} \times 100 \qquad (6)$$

The coefficient of determination (R2), defined as the ratio of explained variation to total variation, serves as a measure of the goodness of fit (Eq.7).

$$R^2 = \frac{\sum (y_i - \bar{y})^2}{\sum (y_i - \bar{y})^2} \qquad (7)$$

## 3.2. ANOVA results for response surface (Ra)

To assess the impact of input parameters in machining processes, Design of Experiments (DOE) was employed, utilizing ANOVA as a statistical method to effectively interpret the experimental data. The coefficient of determination, R2, stands as a pivotal criterion, indicating the ratio of explained variation to total variation, thereby measuring the degree of adjustment. Additionally, R2 (adj) offers an adjusted measure of the model's explanatory power, accounting for the model's complexity.

The analysis, conducted using Design Expert 12, focused on achieving a 95% reliability level or better (P values less than 0.05). Table 3 outlines the results of the variance analysis for the surface roughness criterion Ra. Notably, the most significant factor influencing Ra is the feed rate (fz), contributing to 53.95% of the variation. Increasing the feed rate generates deeper and wider furrows, thereby impacting surface roughness. Following closely is the cutting speed (Vc), contributing 38.75% to the variation. The third most influential factor is fz^2, contributing 2.02%, while the depth of cut (ap) contributes 0.3%. Interactions such as (fz×ap, ap×Vc, and Vc×fz), as well as the effects of products ($Vc^2$ and $ap^2$), were deemed negligible due to their insignificance in the analysis.

**Table 3. Analysis of variance for Ra**

| Source | DF | Seq SS | Adj SS | AdjMS | F | P | Cont% |
|---|---|---|---|---|---|---|---|
| **Regress** | 9 | 38,08 | 38,08 | 4,23 | 19,02 | 0 | 96,61 |
| **Vc** | 1 | 15,28 | 0,05 | 0,05 | 0,2 | 0,02 | 38,75 |
| **fz** | 1 | 21,26 | 2,03 | 2,03 | 9,12 | 0,02 | 53,95 |
| **ap** | 1 | 0,12 | 0,18 | 0,18 | 0,8 | 0,4 | 0,3 |
| **Vc*fz** | 1 | 0,01 | 0,03 | 0,03 | 0,15 | 0,71 | 0,02 |
| **Vc*ap** | 1 | 0,34 | 0,06 | 0,06 | 0,25 | 0,63 | 0,86 |
| **fz*ap** | 1 | 0,23 | 0,08 | 0,08 | 0,35 | 0,57 | 0,59 |
| **Vc*Vc** | 1 | 0,01 | 0 | 0 | 0 | 0,99 | 0,03 |
| **fz*fz** | 1 | 0,8 | 0,81 | 0,81 | 3,64 | 0,1 | 2,02 |
| **ap*ap** | 1 | 0,04 | 0,04 | 0,04 | 0,16 | 0,7 | 0,09 |
| **Error** | 6 | 1,34 | 1,34 | 0,22 | | | |
| **Total** | 15 | 39,42 | | | | | |

Where DF: represent the degree of freedom; SS: represent the sum of squares and MS: adjusted mean squares.

## 3.3. Main effects and interactions

The main effects plot is a valuable tool for analyzing the differences in average responses across different levels of one or more factors. Its significance is heightened when the impact of various factor levels on the response varies. This plot visually represents the mean response for each factor level, connected by lines, providing a clear illustration of the relationships between factors and the response variable.

Upon analysis, the main effects plot highlights the feed rate as the most influential factor, showing the most pronounced trend for roughness Ra in relation to the feed rate. Cutting speed follows closely behind, while the effect of depth of cut shows less significant variation compared to cutting speed and feed rate. This observation is depicted in the main effects diagram of Ra (fig. 4).

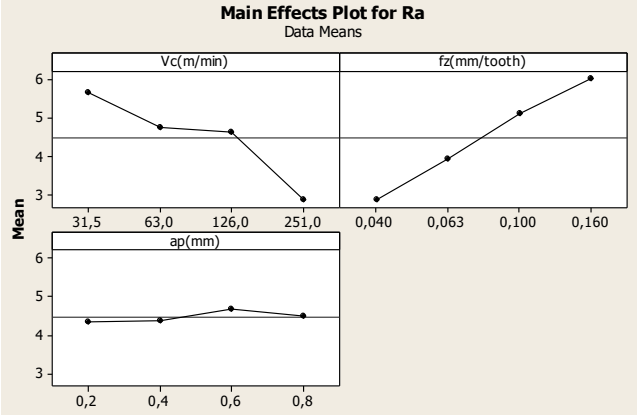


**Fig. 4 A main effects plot representing Ra**

In the interaction diagram, parallel lines indicate the absence of interaction between the two segments, the greater the difference in slope between the lines, the greater the degree of interaction. However, the interaction plot does not indicate whether the interaction is statistically significant (fig. 5).

The relationship between input parameters and performance measurements (outputs) is modeled by quadratic regression using Minitab 16 software.

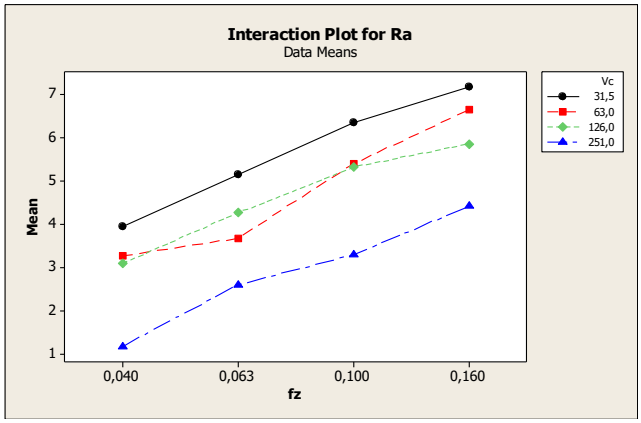


**Fig. 5 An interaction plot illustrating the relationship of Ra**

The regression equation is obtained with determination coefficients (R2). The arithmetic mean roughness (Ra) model and coefficients of determination are given below in equation (8)

**Regression Equation**

$$Ra^2 = -13{,}8153 - 0{,}042332\,Vc + 639{,}517\,fz + 35{,}5878\,ap + 0{,}000274262\,Vc * Vc - 1{,}21604\,Vc * fz - 0{,}0993304\,Vc * ap - 764{,}637\,fz * fz - 278{,}563\,fz * ap - 3{,}08511\,ap * ap \quad (8)$$

With R2=96,61 and Adjusted R2=91,51.

The Residuals plot for Ra includes several representations: a normal probability plot, a histogram of the residuals, Residuals Versus Fitted Values, and Residuals Versus Order of Data, presented in Figure 6. Our observation indicates a good fit of the model in regression and ANOVA analyses, and the normality assumption holds valid.

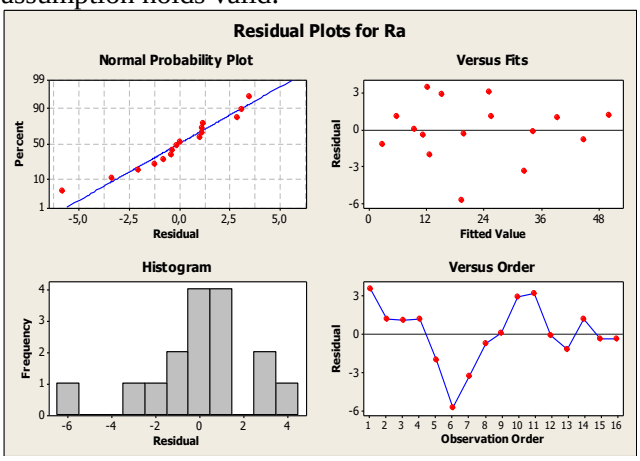


**Fig. 6 Residual plots depicting Ra**

## 3.4. Response surface and contour plots of Ra

The Response surface (Fig. 7) highlights the significant impact of the feed rate, where reducing the feed rate leads to a considerable reduction in surface roughness parameters. Following closely is the cutting speed, which also demonstrates a significant effect, while the depth of cut shows minimal influence. Consequently, optimal surface roughness is achieved by employing a low feed rate and a high cutting speed.

In contrast, the contour graphs (Fig. 8) facilitate the visualization of the response surface and aid in establishing response values. Model verification was conducted through residual analysis, where colored dots represent surface roughness values. The normal probability curves of Ra (Fig. 9) depict residuals closely aligned with the straight line of normality, indicating that errors are normally distributed. Thus, the mathematical models obtained can be reliably utilized for predicting surface roughness.

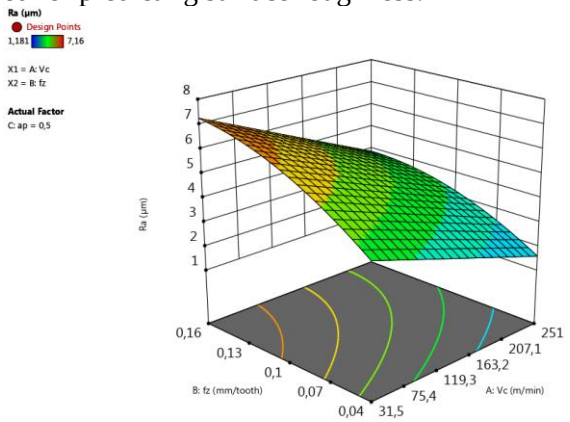


**Fig. 7 A response surface analysis for Ra in relation to Vc, fz, and ap**

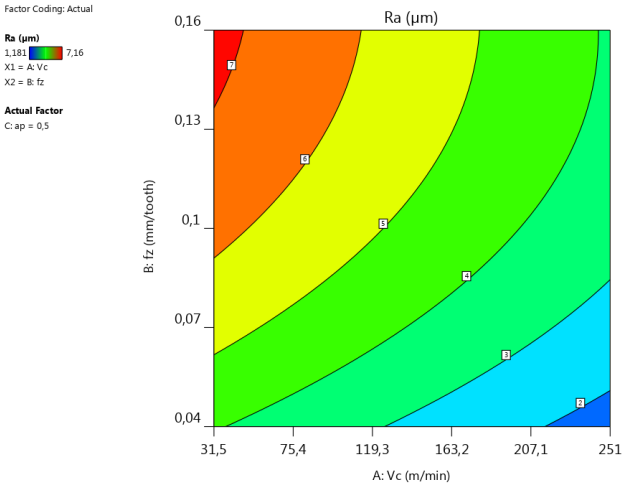


**Fig. 8 A contour plot depicting Ra as a function of Vc, fz, and ap**

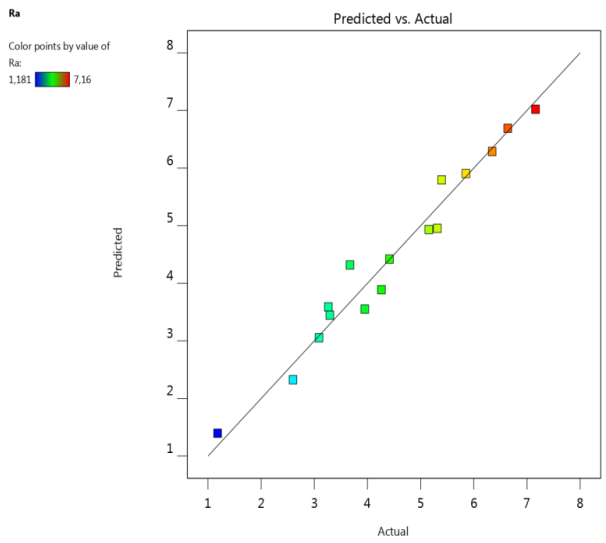


**Fig. 9 The normal probability distribution of Ra**

## 3.5. Multi-response optimization using desirability approach

To attain the optimal machining conditions for milling operations, optimization methods must be employed, considering surface roughness and Material Removal Rate as responses. Material Removal Rate in milling operations refers to the volume of material or metal removed per unit time, measured in mm3/min. This parameter is crucial in manufacturing high-quality products efficiently and cost-effectively within a short timeframe. The Material Removal Rate is calculated using Equation (10).

$$Q = ap \times ae \times fz \times Z \times \frac{Vc \times 1000}{\pi \times D} \qquad (10)$$

To achieve a reduced level of desirability, the optimization results are presented in Figure 10 and Tables 4 and 5. The objective is to minimize Ra (surface roughness) while simultaneously maximizing MRR (Material Removal Rate). The optimal cutting parameters are determined as follows: Vc = 251 m/min, fz = 0.044 mm/tooth, and ap = 0.74 mm. Consequently, the optimized surface roughness and Material Removal Rate are achieved at Ra = 1.604 µm and MRR = 8396 mm3/min, respectively, resulting in a combined desirability of 0.93.

**Table 4. Constraints relevant to optimizing machining parameters**

| Constraints | Goal | Lower limit | Upper limit |
|---|---|---|---|
| Vc | is in range | 31 | 251 |
| fz | is in range | 0,04 | 0,16 |
| ap | is in range | 0,2 | 0,8 |
| Ra | minimize | 1,181 | 7,16 |
| Q | maximize | 707,85 | 8952,87 |

**Table 5. Optimizing responses for surface roughness and MRR**

| Nber | Vc | fz, | ap | Ra, | Q | Desirability |
|---|---|---|---|---|---|---|
| **1** | **251** | **0,044** | **0,74** | **1,604** | **8396** | **Selected 0,93** |
| 2 | 126 | 0,058 | 0,36 | 3,644 | 6198 | 0,62 |
| 3 | 63 | 0,067 | 0,2 | 4,473 | 4659 | 0,46 |
| 4 | 63 | 0,067 | 0,2 | 4,492 | 4699 | 0,46 |

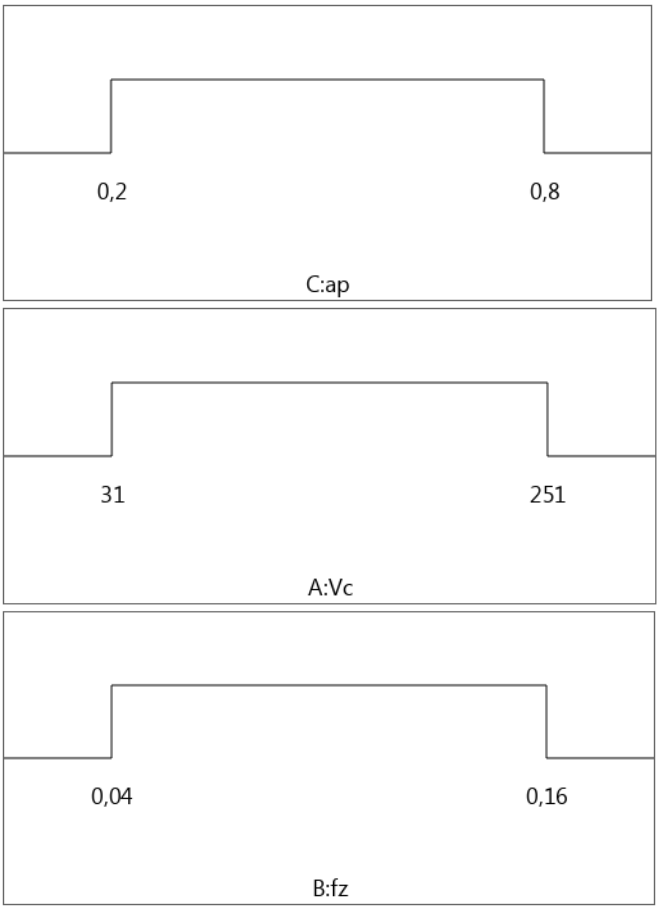

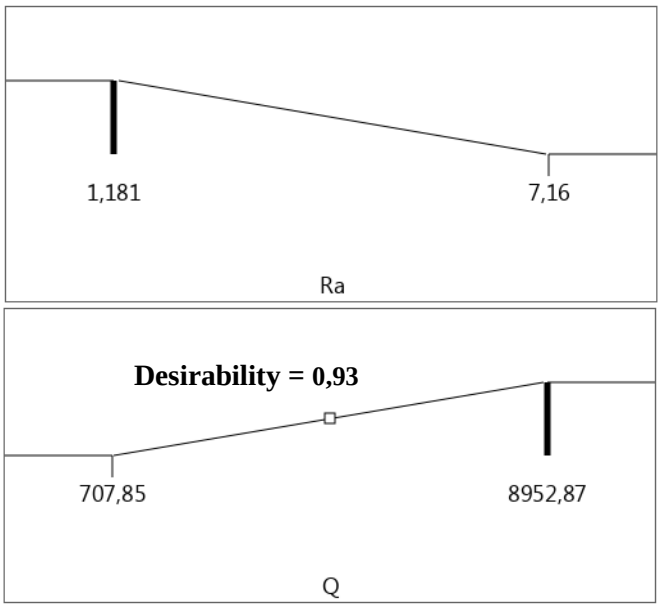


**Fig. 10 Ram function graphs illustrate the relationship between surface roughness and Material Removal Rate**

## 4. CONCLUSIONS

The surfacing tests conducted on 25CrMo4-25 steel utilizing a CT530 cutting insert provided valuable insights into the influence of cutting conditions on roughness Ra and facilitated the development of predictive models. Here are the conclusions drawn from the study:

1 The mathematical model for Ra is highly significant, evidenced by the coefficient of determination R2 = 96.61%.

2 ANOVA analysis indicates that feed rate (fz) significantly affects surface roughness Ra, contributing 53.95%, followed by cutting speed (Vc) with a contribution of 38.75%. However, the depth of cut exhibits a negligible effect. Interactions such as (fz×ap, ap×Vc, and Vc×fz), as well as the effects of products ($Vc^2$ and $ap^2$), were deemed unimportant.

3 Contour plots facilitated the visualization of the response surface in two dimensions, allowing for a comparison of the factors' influence on the response.

4 The mathematical model for Ra is a good representative model, as indicated by the high coefficient of determination R2 of 96.61%. This suggests that surface roughness is closely related to cutting parameters (Vc, fz, and ap) by nearly 100%.

5 Through response surface optimization and the composite desirability method of RSM, optimal cutting parameters for 25CrMo4-25 steel with CT530 inserts were determined: Vc = 251 m/min, fz = 0.044 mm/tooth, and ap = 0.6 mm. The optimized responses are Ra = 1.604 and MRR = 8396 mm3/min, with a composite desirability of 0.93.

## 5. REFERENCES

[1] Lakhdar, B., Athmane, Y. M., Salim, B., & Haddad, A. (2020). Modelling and optimization of machining parameters during hardened steel AISID3 turning using RSM, ANN and DFA techniques: Comparative study. Journal of Mechanical Engineering and Sciences, 14(2), 6835-6847.

[2] Fnides, M., Yallese, M. A., Khattabi, R., Mabrouki, T., &Girardin, F. (2017). Modeling and optimization of surface roughness and productivity thru RSM in face milling of AISI 1040 steel using coated carbide inserts. International Journal of Industrial Engineering Computations, 8(4), 493-512.

[3] Rizvi, S. A., & Ali, W. (2021). Mathematical modelling and optimization of surface roughness and material removal rate during the machining of AISI 1040 steel. Academic Journal of Manufacturing Engineering, 19(3).

[4] Kilickap, E., Yardimeden, A., & Hışman Çelik, Y. (2017). Mathematical modelling and optimization of cutting force, tool wear and surface roughness by using artificial neural network and response surface methodology in milling of Ti-6242S. Applied Sciences, 7(10), 1064.

[5] Laghari, R. A., Li, J., Xie, Z., & Wang, S. Q. (2018). Modeling and optimization of tool wear and surface roughness in turning of Al/SiCp using response surface methodology. 3D Research, 9, 1-13.

[6] Krishnan, B. R. (2020). Review of surface roughness prediction in machining process by using various parameters. International Journal of Recent Trends in Engineering & Research (IJRTER), 6(1), 7-12.

[7] Obilanade, D., Dordlofva, C., & Törlind, P. (2021). Surface roughness considerations in design for additive manufacturing-a literature review. *Proceedings of the design society*, *1*, 2841-2850.

[8] Cabanettes, F., Joubert, A., Chardon, G., Dumas, V., Rech, J., Grosjean, C., & Dimkovski, Z. (2018). Topography of as built surfaces generated in metal additive manufacturing: A multi scale analysis from form to roughness. *Precision Engineering*, *52*, 249-265.

[9] Cao, L., Li, J., Hu, J., Liu, H., Wu, Y., & Zhou, Q. (2021). Optimization of surface roughness and dimensional accuracy in LPBF additive manufacturing. *Optics & Laser Technology*, *142*, 107246.

[10] Khorasani, A., & Yazdi, M. R. S. (2017). Development of a dynamic surface roughness monitoring system based on artificial neural networks (ANN) in milling operation. *The International*

[11] *Journal of Advanced Manufacturing Technology*, *93*, 141-151.

[12] Xie, N., Zhou, J., & Zheng, B. (2018). An energy-based modeling and prediction approach for surface roughness in turning. *The International Journal of Advanced Manufacturing Technology*, *96*, 2293-2306.

[13] Kamguem, R. (2010). Qualité de surface et émissions acoustiques en fraisage haute vitesse des alliages d'aluminium (Doctoral dissertation, École de technologie supérieure).

[14] Chihaoui, S., Yallese, M. A., Belhadi, S., Belbah, A., Safi, K., & Haddad, A. (2021). Coated CBN cutting tool performance in green turning of gray cast iron EN-GJL-250: modeling and optimization. The International Journal of Advanced Manufacturing Technology, 113(11), 3643-3665.

[15] Panwar, V., Sharma, D. K., Kumar, K. P., Jain, A., & Thakar, C. (2021). Experimental investigations and optimization of surface roughness in turning of en 36 alloy steel using response surface methodology and genetic algorithm. *materials today: proceedings*, *46*, 6474-6481.

[16] Sagbas, A. (2011). Analysis and optimization of surface roughness in the ball burnishing process using response surface methodology and desirabilty function. *Advances in Engineering Software*, *42*(11), 992-998.

[17] Yang, A., Han, Y., Pan, Y., Xing, H., & Li, J. (2017). Optimum surface roughness prediction for titanium alloy by adopting response surface methodology. *Results in Physics*, *7*, 1046-1050.

[18] Parida, A. K., & Maity, K. (2019). Modeling of machining parameters affecting flank wear and surface roughness in hot turning of Monel-400 using response surface methodology (RSM). *Measurement*, *137*, 375-381.

[19] Marichamy, S., Saravanan, M., Ravichandran, M., & Stalin, B. (2017). Optimization of surface roughness for duplex brass alloy in EDM using response surface methodology. *Mechanics and Mechanical Engineering*, *21*(1), 57-66.

[20] Bouzid, L., Yallese, M. A., Chaoui, K., Mabrouki, T., &Boulanouar, L. (2015). Mathematical modeling for turning on AISI 420 stainless steel using surface response methodology.Proceedings of the Institution of Mechanical Engineers, Part B: Journal of Engineering Manufacture, 229(1), 45-61.

[21] Palanisamy, A., Jeyaprakash, N., Sivabharathi, V., &Sivasankaran, S. (2022). Effects of dry turning parameters of Incoloy 800H superalloy using Taguchi-based Grey relational analysis and modeling by response surface methodology.Proceedings of the Institution of Mechanical Engineers, Part C: Journal of Mechanical Engineering Science, 236(1), 607-623.

[22] Mohammed, T.H., Montasser, S.T., Joachim, B. (2007). A study of the effects of machining parameters on the surface roughness in the end-milling process. Jordan journal of mechanical and industrial engineering.vol:1, pp 1-5.

[23] Yusuf, K., Nukman, Y., Yusof, T. M. ,Dawal, S. Z. , Qin Yang, H. , Mahlia, T. M. I. and Tamrin, K. F. (2010). Effect of cutting parameters on the surface roughness of titanium alloys using end milling process. Scientific Research and Essays. 5(11), 1284-1293.

[24] Ghosh, G., Mandal, P., &Mondal, S. C. (2019). Modeling and optimization of surface roughness in keyway milling using ANN, genetic algorithm, and particle swarm optimization. The International Journal of Advanced Manufacturing Technology, 100(5), 1223-1242.

[25] Trung, D. D. Influence of cutting parameters on surface roughness during milling AISI 1045 steel. Tribol. Ind. 42 (4), 658–665 (2020).

[26] Kuntoğlu, M., Aslan, A., Pimenov, D. Y., Giasin, K., Mikolajczyk, T., & Sharma, S. (2020). Modeling of cutting parameters and tool geometry for multi-criteria optimization of surface roughness and vibration via response surface methodology in turning of AISI 5140 steel.Materials, 13(19), 4242.

[27] Sureshkumar, B., Vijayan, V., Dinesh, S., &Rajaguru, K. (2019). Neural network modeling for face milling operation.Int J VehStructSyst, 11, 214-219.

[28] Mumtaz, J., Li, Z., Imran, M., Yue, L., Jahanzaib, M., Sarfraz, S., ...&Afzal, K. (2019). Multi-objective optimisation for minimum quantity lubrication assisted milling process based on hybrid response surface methodology and multi-objective genetic algorithm. Advances in Mechanical Engineering, 11(4), 1687814019829588.

[29] Bouzid, L., Boutabba, S., Yallese, M. A., Belhadi, S., &Girardin, F. (2014). Simultaneous optimization of surface roughness and material removal rate for turning of X20Cr13 stainless steel. The International Journal of Advanced Manufacturing Technology, 74(5), 879-891.

[30] Pandiyan, G. K., &Prabaharan, T. (2020). Optimization of machining parameters on AA6351 alloy steel using response surface methodology (RSM).MaterialsToday: Proceedings, 33, 2686-2689.